Proceedings of the 2002 IEEE
International Conference on Robotics & Automation
Washington, DC • May 2002

A New Kind of Singularity in Redundant Manipulation: Semi Algorithmic Singularity

Ki-Cheol Park[1], Pyung-Hun Chang[2], and Sukhan Lee[3]

[1] Institute of Intelligent System, Mechatronics Center, Samsung Electronics Co., Ltd., 416 Maetan-3Dong, Paldal-Gu, Suwon, Kyungki-Do, Korea, 442-742, E-mail: kicheol.park@samsung.com

[2] Department of Mechanical Engineering, KAIST, 373-1 Gusung-Dong, Yusong-Gu, Taejon, Korea. E-mail: phchang@kaist.ac.kr

[3] Samsung Advanced Institute of Technology, Kiheung, Kyungki-do, Korea. E-mail: Lsh@saitgw.sait.samsung.co.kr

Abstract

This paper reports the discovery of a new type of singularity that is as significant as other singularities like kinematic singularity, algorithmic singularity, and semi-singularity. This singularity, named semi algorithmic singularity(SAS), occurs when a redundant manipulator, faced with inequality constraints arising from kinematic limits such as joint angle limits and obstacles, proceeds to conduct optimization of a performance measure.

Through mathematical analysis, we have proved its existence and proposed an analytic matrix function to identify its presence. In conjunction, we have exposed its relationship with the other singularities above. More specifically, SAS is similar to the algorithmic singularity in that it is an artificial singularity coming from an endeavor for performance optimization. They are different in that the former occurs in one direction – among maximization direction and minimization direction – in the C-space, whereas the latter occurs bidirectionally. Besides, we have also found an analogy in the real singularities that while the semi-singularity is unidirectional in the workspace, the kinematic singularity is bi-directional. Through a simulation for a three DOF planar manipulator, we have visualized the existence of SAS and its relationship with the other singularities.

1. Introduction

Our research commenced upon the discovery of a new type of singularity[1] in controlling redundant manipulators. To be more specific, while searching for the optimum joint paths of a seven-degree-of-freedom (DOF) manipulator within the steam generator of a nuclear power plant, we observed that at a particular joint configuration, the manipulator displayed undesirable behaviors such as either sudden stop or rapid self-motions [1]. Upon examination, we were able to determine that this joint configuration did not conform to any existing singularities but was rather a totally new type of singularity. We have designated this singularity as *semi algorithmic singularity* (SAS), and have sought to determine its importance as well as its significance. The following portion will outline the basic foundations for our research.

The discovery of singularities such as kinematic singularity (KS), algorithmic singularity (AS) and semi-singularity (SS) has been well documented. First, kinematic singularity, an indigenous characteristic of the manipulator itself, is a configuration where the end-effector is unable to generate velocity in both a particular direction and its opposite direction within the workspace [2,3]. And algorithmic singularity is a configuration where during the simultaneous conduction of end-effector movement and optimization of the performance measure, the main and secondary tasks become interlocked making simultaneous execution impossible [4,5]. And recently discovered semi-singularity, resulting from kinematic inequality constraints such as obstacles and joint angle limits, is a configuration where the end-effector is unable to generate velocity in a particular direction within the workspace, while still capable of generating velocity in the opposite direction [2,3].

As already known, when a redundant manipulator is subject to these kinds of singularities, the manipulator becomes prone to undesirable responses such as instability and rapid self-motions, which ultimately prevent it from functioning properly. Consequently, understanding these singularities is important, which explains why extensive research aimed at determining their locations through identification or avoiding them altogether has been conducted over the years [2-6,11,15,16].

However, the semi algorithmic singularity presented in this paper is of an entirely new type in that it occurs under circumstances totally different from the aforementioned singularities. SAS occurs in circumstances where both kinematic inequality constraints and optimization of a performance measure should be satisfied simultaneously. Owing to this characteristic, SAS is similar to algorithmic singularity in the sense that the main and secondary tasks of the redundant manipulator cannot be fulfilled simultaneously. However, SAS can be distinguished from algorithmic singularity in the fact that it causes problems in only a *single direction* whether it be the maximization or minimization direction; whereas at algorithmic singularity problems occur in *both directions* regardless of the direction of optimization (maximization or minimization),

The significance of our research lies in the fact that it reports the initial discovery of a new type of singularity, SAS, presents its physical/mathematical implications, and confirms that SAS possesses the same degree of importance as algorithmic singularity. In addition, our research confirms that relationships of SAS with algorithmic singularity are similar to those of semi-singularity with kinematic singularity.

This paper is organized in the following order. Section 2 presents simulation results on semi algorithmic singularity generated occurrences, and explains its physical significance. Section 3 presents the mathematical foundations for semi algorithmic singularity and the analytical function used for its identification. Section 4 reconfirms the existence of semi algorithmic singularity by analyzing its relation with other singularities. Finally, the conclusion is given in Section 5.

[1] In this paper, all joint configurations causing problems during operations by a redundant manipulator are classified as singular points or singularities.

0-7803-7272-7/02/$17.00 © 2002 IEEE

2. Observation Based on Simulation

This section will try to utilize simulation results to effectively portray the singular behavior of a redundant manipulator occurring at semi algorithmic singularity. Semi algorithmic singularity was initially observed from simulations conducted on a spatial 7-DOF manipulator [1]. Visualizing those simulation results, however, proved to be a difficult task, since it requires a complex configuration space analysis. For this reason, we will conduct simulations using a planar 3-DOF manipulator, which is of the most widely used type in redundant manipulator simulations.

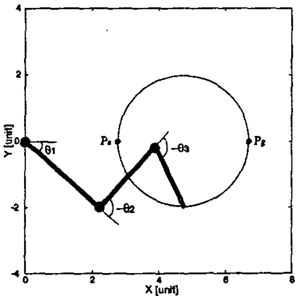

Fig. 1: End-effector path of the manipulator for simulations

As seen in Fig. 1, the manipulator used in the simulation has three links with respective length of 3.0, 2.5, 2.0 units; and its end-effector is supposed to trace a circular trajectory having the center at (4.735,0.000) units and the radius of 1.965 units as follows:

$$x_d(t)=\begin{bmatrix}4.735-1.965\cos(2\pi t)\\ -1.965\sin(2\pi t)\end{bmatrix}. \quad (1)$$

The simulated manipulator is subject to the following kinematic inequality constraints due to the angle limitation of the second joint:

$$60^o \le \theta_2 \le 265^o. \quad (2)$$

At the same time, the manipulator is made to optimize a performance measure, which is the well-known manipulability measure [7]:

$$H(\boldsymbol{\theta})=\sqrt{\det(\boldsymbol{J}\boldsymbol{J}^T)}, \quad (3)$$

where $\boldsymbol{J}$ denotes the Jacobian matrix of the manipulator.

Depending on the direction of optimization, there exists a sort of trade-off relationship for all performance measure results. In the case of manipulability measure, its maximization leads to kinematic singularity avoidance and an increase in motion capability. Whereas its minimization leads to a decrease in motion capability while a corresponding amount of force capability increases [7].

Subsequent simulations will be conducted to compare results when the performance measure optimization direction is either maximized or minimized. To this end, as their initial joint configurations, we have selected local maximum point P_1 and local minimum point P_2 respectively, as follows:

$$\boldsymbol{\theta}_{P_1}(0)=\left[\text{-9.56}^\circ \quad 102.36^\circ \quad 175.30^\circ\right]^T, \quad (4)$$

$$\boldsymbol{\theta}_{P_2}(0)=\left[\text{-14.35}^\circ \quad 156.47^\circ \quad \text{-165.43}^\circ\right]^T. \quad (5)$$

Needless to say, the main task for both cases is to avoid joint angle limits while ensuring that the end-effector follows the circular trajectory (1).

The control methods for this redundant manipulator need to be capable of simultaneously managing both kinematic inequality constraint conditions and performance measure optimization. Two of typical control methods that meet these requirements may be Sung's method [8] and the compact quadratic programming method (CQPM) [9]. Note that Sung's method may be regarded as a generalization for the extended Jacobian method (EJM) [4,5] that covers the case with kinematic inequality constraint conditions, whereas CQPM the same generalization for resolved motion rate control (RMRC) [10]. Owing to space limitations, introduction of these methods have been omitted in this paper.

Fig. 2 and 3 present the respective simulation results when applying Sung's method and the compact quadratic programming method to conduct main and secondary tasks simultaneously. The left and right columns for each figure show the results for cases of maximizing and minimizing the measure, respectively, while the upper and lower rows present joint angle trajectory and results of its projection onto a configuration space (C-space) $\theta_2-\theta_3$ plane. To be more specific, the shaded regions in the lower rows represent impenetrable zones caused by joint angle limits while the dashed and dotted lines each represent self motion manifolds (SMM) [11] for workspace points P_s and P_g in Fig. 1.

Observing the results for application of Sung's method in Fig. 2, for maximization (left column), the manipulator proceeds from P_1 and stops at P_a. For minimization (right column), the manipulator proceeds from P_2 and passes the same configuration P_a without experiencing any problems and accomplishes all objectives with repeatability.

As for the application results of the compact quadratic programming method, they are similar to those of Sung's method as seen in Fig. 3. For maximization (left column), the manipulator proceeds from P_1, rapidly jumps at P_a to a different configuration through self-motion, and did not return to the original joint configuration, revealing the repeatability problem. In contrast, for minimization (right column), it passes the same configuration P_a without experiencing any problems and accomplishes all objectives with repeatability.

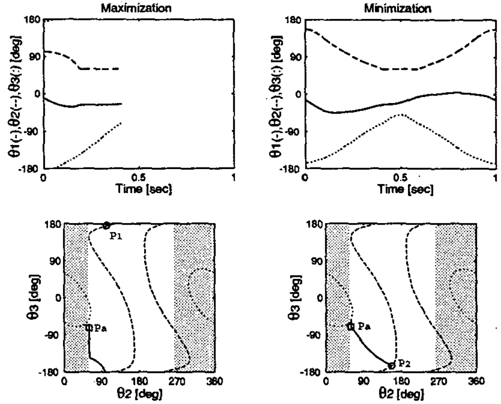

Fig. 2: Simulation results of Sung's method

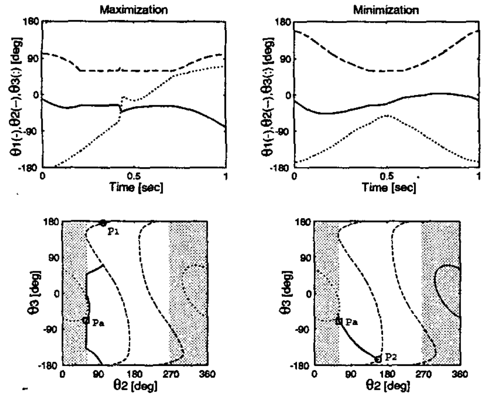

Fig. 3: Simulation results of the CQPM

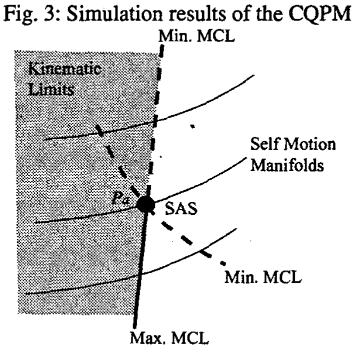

Fig. 4: Conceptual figure for P_a (SAS) on C-space

In order to understand the phenomena occurring at joint configuration P_a, we need to consider the physical characteristics surrounding the area along with analysis of the joint configuration itself. In Fig. 4, with the focus being configuration P_a, the maximum (thick solid lines) and minimum values (thin solid line), obtained from kinematic limits, self-motion manifolds, and simulation results, are marked in the C-space. These values are designated as maximum measure constraint loci (MCL) and minimum measure constraint loci [12], respectively, since the maximum and minimum values form a series of loci. From P_a, there exists a max. MCL and min. MCL along the lower and upper boundary of the kinematic limit, respectively, while another min. MCL exists crossing the boundary of the kinematic limit. In other words, P_a is the spot where the maximum and minimum solution loci meet one another.

The main task of the manipulator, the end-effector movement, can be represented as the configuration change in the C-space, from one self-motion manifold to a different one within the joint angle limit. If the secondary objective is to maximize the performance measure, then we can no longer move the manipulator upwards to a different self-motion manifold from P_a. However, if minimization is the objective, then P_a does not become a problematic configuration. And if optimization of the performance measure is not considered, we can proceed to move the manipulator to another self-motion manifold from P_a without encountering any problematic configurations. It can be said that these situations occur when performance measure optimization is conducted, and that, along the boundaries of kinematic limits, algorithmic singularity is evident only for a uni-direction of optimization. Because of this fact, P_a is designated as a semi algorithmic singularity.

Thus, semi algorithmic singularity displays unique characteristics different to other existing singularities. In order to further determine the cause of these characteristics, we generalize semi algorithmic singularity through its mathematical analysis. In the following section, we will present the necessary mathematical evidence.

3. Mathematical Foundation

In this section, we will present the mathematical foundations for semi algorithmic singularity and in the process obtain its identification measure. For this, we will briefly introduce the constrained optimization problem and the necessary condition for optimization.

Based on the nonlinear optimization theory [13], the manipulator redundancy resolution problem with multiple subtasks has been formulated into the general problem of local constrained optimization under kinematic inequality constraints [8,9] as follows:

$$\text{maximize (or minimize) } H(\boldsymbol{\theta})$$
$$\text{subject to } \boldsymbol{f}(\boldsymbol{\theta}) = \boldsymbol{x} \text{ and } \boldsymbol{g}(\boldsymbol{\theta}) \le 0, \tag{6}$$

where $\boldsymbol{f}(\boldsymbol{\theta})$ denotes the m-dimensional kinematic function vector and $\boldsymbol{g}(\boldsymbol{\theta})$ denotes a p-dimensional vector for describing kinematic limits such as joint angle limits and obstacles.

The general constrained optimization problem (6) has already been solved by using the necessary conditions in [13], which are briefly reviewed in this section through Theorem 1. Note that the theorem uses the Lagrangian function given as follows:

$$L(\boldsymbol{\theta}, \boldsymbol{\lambda}, \boldsymbol{\mu}) = H(\boldsymbol{\theta}) + \boldsymbol{\lambda}^T \boldsymbol{f}(\boldsymbol{\theta}) + \boldsymbol{\mu}^T \boldsymbol{g}(\boldsymbol{\theta}), \tag{7}$$

where $\boldsymbol{\lambda}$ and $\boldsymbol{\mu}$ denote m and p-dimensional Lagrange multiplier vectors, respectively.

Theorem 1 (Kuhn-Tucker conditions or the necessary conditions for constrained maximization (or minimization)[13]): Let $\boldsymbol{\theta}^*$ be a local maximum (or minimum) configuration for the problem (6) and suppose $\boldsymbol{\theta}^*$ is a non-singular configuration for the constraints. Then there exist a vector $\boldsymbol{\lambda} \in \Re^p$ and a vector $\boldsymbol{\mu} \in \Re^p$ with $\boldsymbol{\mu} \le (\text{or } \ge) \boldsymbol{0}$ such that

$$\nabla L(\boldsymbol{\theta}^*) = \nabla H(\boldsymbol{\theta}^*) + \boldsymbol{\lambda}^T \nabla \boldsymbol{f}(\boldsymbol{\theta}^*) + \boldsymbol{\mu}^T \nabla \boldsymbol{g}(\boldsymbol{\theta}^*) = \boldsymbol{0} \in \Re^n, \tag{8}$$

$$\boldsymbol{\mu}^T \boldsymbol{g}(\boldsymbol{\theta}^*) = 0 \in \Re^1, \tag{9}$$

where $\nabla(\cdot)$ denotes $\frac{\partial}{\partial \theta}(\cdot)$.

Proof: see [13].

Observing the simulation results in Section 2, semi algorithmic singularity occurs at the joint configuration where the direction of optimization changes after following the boundaries of kinematic limits. To be more specific, Sung's method is an algorithm derived directly from the Kuhn-Tucker necessary condition [8]. And the fact that Sung's method ceases to function when encountering semi algorithmic singularity, indicates that the Kuhn-Tucker necessary condition is no longer satisfied once it passes the spot of semi algorithmic singularity. In this section, we will seek to present the mathematical foundations of semi algorithmic singularity through the confirmation of the Kuhn-Tucker necessary condition in the situation mentioned above.

The fact that an optimization value exists along a certain kinematic limit boundary indicates that the following set exists:

$$B=\left\{ i \mid G_i(\boldsymbol{\theta}^*)=0 \right\}. \tag{10}$$

Here, $G_i(\boldsymbol{\theta}^*)$ denotes the i -th scalar element of vector $\boldsymbol{g}(\boldsymbol{\theta}^*)$. Then, depending on whether it belongs to set B, $G_i(\boldsymbol{\theta}^*)$ can be classified as either case $G_i(\boldsymbol{\theta}^*)=0\,(i\in B)$ or case $G_i(\boldsymbol{\theta}^*)<0\,(i\notin B)$. Next, μ_i, which denotes the i -th scalar element of the Lagrange multiplier vector $\boldsymbol{\mu}$, can be classified as the following 4 cases using the Kuhn-Tucker necessary condition (9): $[\mu_i=0\,,i\notin B]$, $[\mu_i=0\,,i\in B]$, $[\mu_i<0\,,i\in B]$, and $[\mu_i>0\,,i\in B]$, which is shown well in Fig. 5. Here, it is helpful to note that $[\mu_i=0\,,i\in B]$ exists along the boundaries of the other 3 conditions: $[\mu_i=0\,,i\notin B]$, $[\mu_i<0\,,i\in B]$, and $[\mu_i>0\,,i\in B]$.

By observing the Kuhn-Tucker necessary condition, we can detect that the signs of the Lagrange multiplier vector $\boldsymbol{\mu}$, differ greatly according to the direction (maximization/ minimization) of optimization. In other words, according to the Kuhn-Tucker necessary condition, $[\mu_i\le 0\,,i\in B]$ and $[\mu_i\ge 0\,,i\in B]$ are the respective necessary conditions for maximization and minimization. And $[\mu_i=0\,,i\in B]$ can become the necessary condition for both maximization and minimization. Therefore, it can be said that the maximum and minimum values diverge at configuration $[\mu_i=0\,,i\in B]$, and that this configuration is identical to the semi algorithmic singularity we discovered.

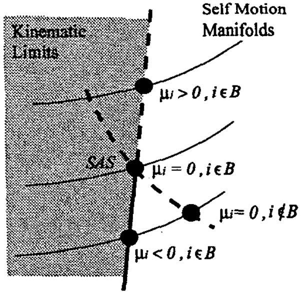

Fig. 5: Conceptual figure for 4 cases of μ_i on C-space

Now, using $[\mu_i=0\,,i\in B]$, we will obtain the sole analytic function of $\boldsymbol{\theta}^*$. First, $\boldsymbol{g}_b$ is defined as a vector with an element of $G_i(i\in B)$ and $\boldsymbol{\mu}_b$ is defined as a Lagrange vector related to $\boldsymbol{g}_b$ and satisfying $\boldsymbol{\mu}_b^T\boldsymbol{g}_b=0$. Then (8) is expressed as the following:

$$\nabla H+\boldsymbol{\lambda}^T\nabla \boldsymbol{f}+\boldsymbol{\mu}_b^T\nabla \boldsymbol{g}_b=\boldsymbol{0}. \tag{11}$$

When assuming transpose to both sides of the equation (11), the following is obtained:

$$\boldsymbol{h}+\boldsymbol{J}^T\boldsymbol{\lambda}+\nabla\boldsymbol{g}_b^T\boldsymbol{\mu}_b=\boldsymbol{0}, \tag{12}$$

where $\boldsymbol{h}=\left(\nabla H\right)^T$ and $\boldsymbol{J}=\nabla \boldsymbol{f}$. And then by multiplying $\boldsymbol{Z}$, the null space matrix of $\boldsymbol{J}$, to both sides of the equation (12) and by arranging the equation, we obtain the following

$$\boldsymbol{Z}\nabla\boldsymbol{g}_b^T\boldsymbol{\mu}_b=-\boldsymbol{Zh} \tag{13}$$

because of $\boldsymbol{ZJ}^T=\boldsymbol{0}$. Then, by multiplying $\nabla\boldsymbol{g}_b\boldsymbol{Z}^T$ to both sides of the equation (13), we obtain the following:

$$\nabla\boldsymbol{g}_b\boldsymbol{Z}^T\boldsymbol{Z}\nabla\boldsymbol{g}_b^T\boldsymbol{\mu}_b=-\nabla\boldsymbol{g}_b\boldsymbol{Z}^T\boldsymbol{Zh}. \tag{14}$$

Then $\boldsymbol{\mu}_b$ is obtained as follows:

$$\boldsymbol{\mu}_b(\boldsymbol{\theta}^*)=-\left(\nabla\boldsymbol{g}_b\boldsymbol{Z}^T\boldsymbol{Z}\nabla\boldsymbol{g}_b^T\right)^{-1}\nabla\boldsymbol{g}_b\boldsymbol{Z}^T\boldsymbol{Zh}. \tag{15}$$

Here, we define a new matrix function, $\boldsymbol{C}_{SAS}\equiv\text{diagonal}\left(\boldsymbol{\mu}_b\right)$. Then the following square matrix function can be finally obtained

$$\boldsymbol{C}_{SAS}(\boldsymbol{\theta}^*)=\text{diagonal}\left(-\left(\nabla\boldsymbol{g}_b\boldsymbol{Z}^T\boldsymbol{Z}\nabla\boldsymbol{g}_b{}^T\right)^{-1}\nabla\boldsymbol{g}_b\boldsymbol{Z}^T\boldsymbol{Zh}\right). \tag{16}$$

Ultimately, the semi algorithmic singularity condition of $[\mu_i=0\,,i\in B]$ is identical to the singular case of the matrix function $\boldsymbol{C}_{SAS}(\boldsymbol{\theta}^*)$. Consequently, $\boldsymbol{C}_{SAS}(\boldsymbol{\theta}^*)$ denotes the analytic function for identifying the semi algorithmic singularity.

If then, what is the relationship of semi algorithmic singularity with other singularities? We will address this issue in the following section by comparing its physical and mathematical significance.

4. Relationships with Other Singularities

In this section, we will examine the relationship of singularities other than semi algorithmic singularity such as kinematic singularity, semi-singularity, and algorithmic singularity. In order to visualize the respective characteristics of each, we will use a conceptual figure within C-space. The redundant manipulator deployed for this conceptual figure is the planar 3-DOF manipulator identical to the one used for simulation in Section 2.

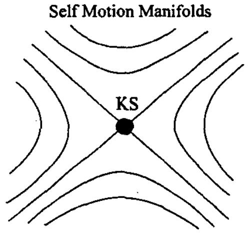

Fig. 6: kinematic singularity on C-space

As shown in Fig. 6, kinematic singularity[2] is situated at the configuration where two or more self-motion manifolds intercross within C-space [11]. Since it is possible from this configuration to change configurations in several directions while

[2] Kinematic singularity here means only internal kinematic singularity. External kinematic singularity is located at the boundary of the workspace and does not allow any self-motion, thus self-motion manifold are designated as a point in C-space.

moving along a self-motion manifold, we can effectively avoid kinematic singularity by controlling self-motion [11]. However, while this leads to an increase in the degree of freedom for self-motion occurring directly above kinematic singularity, it results in a decrease in a corresponding degree of freedom within the workspace [14]. Consequently, particular bi-directional movement within the workspace is impossible to achieve from this configuration [2,3]. Kinematic singularity can be easily identified through the singularity of the Jacobian matrix [4], which is given as the following square matrix function.

$$C_{KS} = JJ^T \tag{17}$$

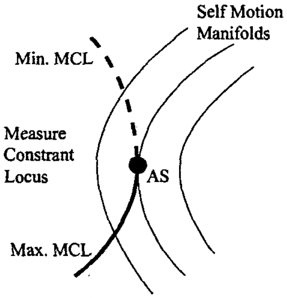

Fig. 7: Algorithmic singularity (AS) on C-space

As illustrated in Fig. 7, algorithmic singularity always occurs at a point where a self-motion manifold is tangent to the measure constraint locus (MCL) [15,16]. In order to perform the main task, movement from one self-motion manifold to another must be accomplished, and for the secondary task, maintaining of the optimum value trajectory (MCL) is essential. However, simultaneous conduction of the main and secondary tasks becomes impossible beyond the point of contact where the measure constraint locus and self-motion manifold meet. This configuration can be defined as algorithmic singularity since an algorithm incurs it [15,16]. Algorithmic singularity can be identified by the following square matrix function [15,16].

$$C_{AS} = \nabla(Zh)Z^T \tag{18}$$

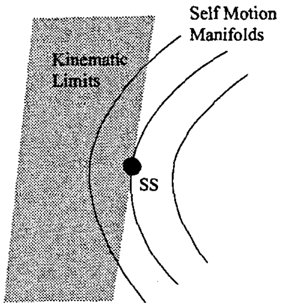

Fig. 8: Semi-singularity (SS) on C-space

As for the recently discovered semi-singularity, it possesses the same level of importance as kinematic singularity with the viewpoint of self-motion topology and global path planning [2,3]. Observing Fig. 8, semi-singularity always occurs at a point on the boundary of kinematic limits where a self-motion manifold is tangent to such a boundary [2,3]. While semi-singularity prevents end-effector movement in a particular direction within the workspace, this configuration enables movement in the opposite direction [2,3]. In other words, kinematic singularity is bi-directional whereas semi-singularity is uni-directional [2,3]. The term semi-singularity is derived from this characteristic, however, when considering its physical aspects, semi kinematic singularity should be a more accurate term. Determining the singularity of the following square matrix function can identify semi-singularity[3] [3].

$$C_{SS} = \nabla g_b Z^T Z \nabla g_b^T \tag{19}$$

Fig. 9 explains the various joint configurations from which the 4 types of singularities occur in the planar 3-DOF manipulator during simulation of Section 2. Analyzing the results, we can determine that these singularities are derived from the correlation among self-motion manifolds (thin solid line), kinematic limits (shaded region), maximum measure constraint loci (thick solid line), and minimum measure constraint loci (thick dashed line). The maximum and minimum measure constraint loci in Fig. 9 are obtained by using the respective necessary and sufficient conditions [13] for maximization and minimization, respectively. We can observe that at the borders of the maximum and minimum solution loci, there exist 3 kinematic singularities (filled circles), 4 semi-singularities (blank circles), 8 algorithmic singularities (filled squares), and 8 semi algorithmic singularities (blank squares). To be more specific, while following the maximum (or minimum) measure constraint loci, there is bound to exist one of the 4 types of singularities at the spot where further compliance to the maximum (or minimum) solutions is no longer possible. Therefore, upon encountering any one of the 4 types of singularities mentioned above when using a redundant manipulator, under optimum control conditions, to track maximum (minimum) solutions, the manipulator ceases to follow the maximum (minimum) solutions and depending on the control methods, experiences singular behaviors such as break-down, rapid self-motion and sudden stop.

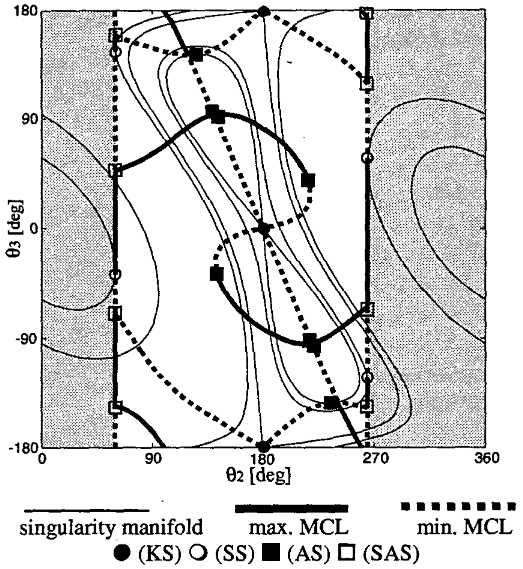

Fig. 9: Locations of singularities of the simulated manipulator on C-space

It is noteworthy that each and all of the 4 types of singularities,

[3] Semi-singularity includes both smooth tangency case and non-smooth tangency case. Without loss of generality, in this paper, we consider only smooth tangency case.

kinematic singularity, semi-singularity, algorithmic singularity and semi algorithmic singularity, occurred under different circumstances. In cases where only the kinematic equation – the equality constraint – is considered, there exists only kinematic singularity. If we include performance optimization along with the kinematic equation, then algorithmic singularity occurs in addition to kinematic singularity. Also, if kinematic limits – kinematic inequality constraints – exist without any performance optimization, only semi-singularity occurs in addition to kinematic singularity. Finally, if both kinematic inequality constraints and performance optimization are considered simultaneously, then all the types of singularities (KS, SS, AS, and SAS) become present. It is also noteworthy that SAS occurs only when we have all the three circumstances together: kinematic equation, kinematic limit and performance optimization. In our opinion, it is for this reason that semi algorithmic singularity was the last singularity to be discovered.

In addition to these facts, kinematic singularity and semi-singularity are caused by mechanical kinematics and may be classified as *real singularity*. In contrast, algorithmic singularity and semi algorithmic singularity are caused by performance measure optimization and thus may be categorized as *artificial singularity*. Also, since kinematic singularity and algorithmic singularity are caused solely by equality constraints, they are *bi-directional*, whereas semi-singularity and semi algorithmic singularity, being caused by inequality constraints, become *uni-directional*. This relationship is illustrated in Table 1. Of course, directionality for kinematic singularity and semi-singularity implies to the direction *in the workspace*, whereas directionality for algorithmic singularity and semi algorithmic singularity implies to direction of *optimization (max/min)*. However, it appears a natural analogy that as there exists semi-singularity possessing properties of reality and uni-directionality, so exists semi algorithmic singularity having properties of artificiality and uni-directionality.

Table 1: Properties of Singularities

	bi-directional	uni-directional
real singularity	KS	SS (=SKS)
artificial singularity	AS	**SAS**

Besides the aforementioned method for determining the existence of semi algorithmic singularity, *to avoid its occurrence* is another major task, which is beyond the intended scope of this paper and will be covered in a subsequent paper.

5. Conclusion

The objective of this paper was to report a new type of singularity, *semi algorithmic singularity*, during control of a redundant manipulator, and to explain the importance and significance of this new discovery. Semi algorithmic singularity occurs when a redundant manipulator, faced with inequality constraints arising from kinematic limits such as joint angle limits and obstacles, proceeds to conduct optimization of a performance measure.

Through simulation results for a planar 3-axis manipulator and mathematical analysis, the existence of SAS was reconfirmed. In addition, as the result of mathematical analysis, an analytic matrix function has been proposed to identify its presence.

Furthermore, we have investigated its relationship with other singularities such as kinematic singularity, algorithmic singularity, and semi singularity. As a result, we have shown that just as semi-singularity is derived from kinematic singularity, so was SAS from algorithmic singularity. In other words, we confirmed that natural analogy played a role in the existence of singularities.

In conclusion, through this paper, we were able to analyze all types of singularities occurring when optimal control of a redundant manipulator was being conducted. We believe that this knowledge can contribute to the optimal control of various types of redundant manipulators.

References

[1] K.C. Park, P.H. Chang, and J.K. Salisbury, "A Unified Approach for Local Resolution of Kinematic Redundancy with Inequality Constraints and Its Application to Nuclear Power Plant," in *Proc. IEEE ICRA*, pp.766-773, 1997.

[2] C.L. Luck and S. Lee, "Self-Motion Topology for Redundant Manipulators with Joint Limits," in *Proc. IEEE ICRA*, pp.626-631, 1993.

[3] C.L. Luck and S. Lee, "Redundant Manipulators under Kinematic Constraints: A Topology-Based Kinematic Map Generation and Discretization," in *Proc. IEEE ICRA*, pp.1-6, 1995.

[4] J. Bailieul, "Kinematic Programming Alternatives for Redundant Manipulators," *Proc. IEEE Int. Conf. Robotics and Automation*, pp. 722-728, 1985.

[5] J. Bailieul, "Avoiding Obstacles and Resolving Kinematic Redundancy," *Proc. IEEE Int. Conf. Robotics and Automation*, pp. 1698-1704, 1986.

[6] D.N. Nenchev, "Redundancy Resolution through Local Optimization: A Review," *J. Robotic Systems*, vol.6, no.6, pp.769-798, 1989.

[7] T. Yoshikawa, "Manipulability of Robotic Mechanism," *Int. J. Robotics Res*. vol..4, no.2, pp.3-9, 1985

[8] Y.W. Sung, D.K. Cho, and M.J. Chung, "A Constrained Optimization Approach to Resolving Manipulator Redundancy," J. Robotic Systems, vol.13, no.5, pp.275-288, 1996.

[9] F.-T. Cheng, T.-H. Chen, and Y.-Y. Sun, "Resolving Manipulator Redundancy Under Inequality Constraints," *IEEE Trans. Robotics Automat.*, vol.10, no.1, pp.65-71, Feb. 1994.

[10] D.E. Whitney, "Resolved Motion Rate Control of Manipulators and Human Prosthesis," *IEEE Trans. Man-Machine Systems*, vol.MMS-10, no.2, pp.47-53, 1969.

[11] J.W. Burdick, "On the Inverse Kinematics of Redundant Manipulators: Characterizations of the Self-Motion Manifold," in *Proc. IEEE ICRA*, pp. 264-270, 1989.

[12] B.W. Choi, J.H. Won, and M.J. Chung, "Manipulability Constraint Locus for a Redundant Manipulator," in *Proc. IEEE/RSJ IROS*, pp.167-172, 1991.

[13] D.G. Luenberger, *Linear and Nonlinear Programming*, 2nd ed. Addison-Wesley Publishing Company, 1984.

[14] Y. Nakamura, *Advanced Robotics: Redundancy and Optimization*, Addison-Wesley Publishing Company, 1991.

[15] D.K. Cho, B.W. Choi, and M.J. Chung, "Optimal Conditions for Inverse Kinematics of a Robot manipulator with redundancy," *Robotica*, vol.13, pp.95-101, 1995.

[16] J. Park, W.-K. Chung, and Y. Youm, "Characteristics of Optimal Solutions in Kinematic Resolutions of Redundancy," *IEEE Trans. R & A*, vol.12, no.3, pp.471-478, 1996.